a reprint from Applied Optics

Four-stream solution for atmospheric radiative transfer over a non-Lambertian surface

Shunlin Liang and Alan H. Strahler

An analytical model characterizing the atmospheric radiance field over a non-Lambertian surface divides the radiation field into three components: unscattered radiance, single-scattering radiance, and multiple-scattering radiance. The first two components are calculated exactly. A δ-four-stream approximation is extended to calculate the azimuth-independent multiple-scattering radiance over a non-Lambertian surface, which is modeled by a statistical bidirectional reflectance distribution function (BRDF). Accuracy is assessed with respect to the exact results computed from a Gauss–Seidel iterative algorithm. Experiments comparing the results obtained with Lambertian and non-Lambertian surfaces show that incorporating the BRDF into the four-stream approximation significantly improves the accuracy in calculating radiance as well as radiative flux.

Key words: Radiative transfer, atmospheric optics, four-stream, remote sensing.

1. Introduction

Most land surfaces are strongly anisotropic reflectors at optical wavelengths. The primary source of this anistropy is the three-dimensional structure of the surface. A number of instruments that can remotely sense the anisotropy of the land surface are now available or are in development. Examples are the Advanced Solid-State Array Spectroradiometer,[1] a pointable, aircraft-mounted imaging spectroradiometer, and the Multiangle Imaging Spectroradiometer (MISR),[2] proposed as part of NASA's Earth Observing System. To retrieve ground structural information effectively from multiangle remotely sensed data, which is a requirement for global climatic modeling or ecosystem studies, we need to develop simple and accurate analytical models that characterize the angular atmospheric radiation field over a non-Lambertian surface.

Radiative transfer theory is a powerful tool to model atmospheric radiation characteristics. Many numerical models have been reported in the literature.[3–7] Unfortunately these models are undesirable for inversion purposes because they require extensive calculations. To retrieve surface structural information or directional reflectance, optimum algorithms that involve hundreds or even thousands of such forward calculations are frequently used. Fast algorithms are required for this purpose. The two-stream approximation, which is simple to calculate and is widely used in radiative flux transfer modeling, recently has been extended to calculate the angular radiance field when considering a non-Lambertian surface as the lower boundary condition.[8] Two-stream Kubelka–Munk theory has also been extended to apply to the scene-radiation modeling.[9] However, if high accuracy is required, it is desirable to explore new models that are still simple but more accurate. The four-stream approximation, used in radiative flux calculation over a Lambertian surface,[10–12] is a good candidate. A procedure for calculating the angular radiance of the atmosphere over a non-Lambertian surface by means of the four-stream approximation provides the focus of this paper.

To evaluate the angular characteristics as accurately as possible, the radiation field is divided into three components: solar radiance that is unscattered by the atmosphere, single-scattering radiance, and multiple-scattering radiance. The first two components can be calculated exactly. Only the multiple-scattering component is approximated by the use of the δ-four-stream solution. The accuracy of this

S. Liang is with the Department of Geography, University of Maryland, College Park, Maryland 20742. A. H. Strahler is with the Center for Remote Sensing and the Department of Geography, Boston University, 725 Commonwealth Avenue, Boston, Massachusetts 02215.

Received 25 January 1993; revised manuscript received 16 March 1994.

0003-6935/94/245745-09$06.00/0.

approximation for aerosol atmospheres is checked with the Gauss–Seidel iterative code.[7]

2. Decomposition of the Radiation Field

For a plane-parallel homogeneous atmosphere in the absence of polarization, the radiative transfer equation can be written as[13]

$$\mu \frac{\partial I(\tau, \Omega)}{\partial \tau} = I(\tau, \Omega) - \frac{\omega}{4\pi} \int_{4\pi} P(\Omega', \Omega) I(\tau, \Omega') \mathrm{d}\Omega', \quad (1)$$

subject to the boundary conditions

$$\begin{cases} I(0, \Omega) = \delta(\Omega - \Omega_0)\pi F_0 \\ I(\tau_0, \Omega) = \displaystyle\int_{2\pi-} R(\Omega', \Omega)|\mu'| I(\tau_0, \Omega')\mathrm{d}\Omega', \end{cases}$$

where ω is the single-scattering albedo, F_0 is the extraterrestrial irradiance, $P(\Omega', \Omega)$ is the phase function, $\delta(\cdot)$ is the Dirac delta function, $R(\Omega', \Omega)$ is the ground bidirectional reflectance distribution function (BRDF), and τ is the optical depth varying from zero at the top of the atmosphere to τ_0 at the bottom of the atmosphere. The direction $\Omega(\mu, \phi)$ characterizes azimuthal angle ϕ and zenith angle $\theta = \cos^{-1}(\mu)$, for which a negative μ indicates the downward direction and a positive μ indicates the upward direction. Ω_0 denotes the solar incident direction with the zenith angle $\theta_0 = \cos^{-1}(|\mu_0|)$ and the azimuth angle ϕ_0. Because $|\mu_0|$ is so frequently below, it is replaced with μ_0 for convenience.

The scattering properties of the atmosphere depend on Rayleigh and aerosol particles. Thus the scattering-phase function can be defined as a weighted average of individual scattering-phase functions at a specific scattering angle:

$$P(\Psi) = \frac{p_r(\Psi)\tau_r + p_a(\Psi)\tau_a}{\tau_r + \tau_a},$$

with the constraint $\frac{1}{2}\int_0^\pi P(\Psi)\sin\Psi \mathrm{d}\Psi = 1$. Here Ψ is the scattering angle, dependent on the incident zenith angle, the viewing angle, and the azimuth angle difference. τ_r and τ_a are the molecular optical depth and aerosol optical depth, respectively. The one-term Henyey–Greenstein function is used as the aerosol phase function.

It is well known that no analytic solution to Eq. (1) can be obtained. To incorporate a non-Lambertian surface into the four-stream approximation and obtain a more exact angular dependence of the radiance, we divide the radiation field into three components: unscattered solar radiance (us), single-scattering radiance (ss), and multiple-scattering (ms). The multiple-scattering radiance $I^{\mathrm{ms}}(\tau, \mu)$ is assumed to be azimuthally independent. For the us and ss components, the formulas are quite simple. When $\mu > 0$,

$$I^{\mathrm{us}}(\tau, \Omega) = \pi F_0 \mu_0 R(\Omega_0, \Omega) \exp\left(-\frac{\tau_0}{\mu_0} - \frac{\tau_0 - \tau}{\mu}\right),$$

$$I^{\mathrm{ss}}(\tau, \Omega) = \frac{\omega F_0 P(\Omega_0, \Omega)\mu_0}{4(\mu_0 + \mu)} \left\{\exp\left(-\frac{\tau}{\mu_0}\right) - \exp\left[\frac{\tau}{\mu} - \tau_0\left(\frac{1}{\mu_0} + \frac{1}{\mu}\right)\right]\right\}. \quad (2)$$

When $\mu < 0$,

$$I^{\mathrm{us}}(\tau, \Omega) = \pi F_0 \delta(\Omega - \Omega_0) \exp\left(-\frac{\tau}{\mu_0}\right),$$

$$I^{\mathrm{ss}}(\tau, \Omega) = \frac{\mu_0 F_0 \omega P(\Omega_0, \Omega)}{4(\mu_0 - |\mu|)} \left[\exp\left(-\frac{\tau}{\mu_0}\right) - \exp\left(-\frac{\tau}{|\mu|}\right)\right], \quad |\mu| \neq \mu_0,$$

$$I^{\mathrm{ss}}(\tau, \Omega) = \frac{\omega F_0 \tau}{4\mu_0} P(\Omega_0, \Omega) \exp\left(-\frac{\tau}{\mu_0}\right), \quad |\mu| = \mu_0. \quad (3)$$

3. Four-Stream Approximation for Multiple Scattering

Because the formulas for the multiple-scattering radiance cannot be explicitly derived, here we use the four-stream approximation. If the unscattered radiance from Eq. (1) is decomposed, the corresponding equation for the scattering radiance will have one more source term contributed by the unscattered radiance. The azimuth-independent radiative transfer equation for the total scattering radiance is

$$\mu \frac{\mathrm{d}I(\tau, \mu)}{\mathrm{d}\tau} = I(\tau, \mu) - \frac{\omega}{2} \int_{-1}^{1} p(\mu, \mu') I(\tau, \mu') \mathrm{d}\mu' - \frac{\omega}{4} F_0 p(\mu, -\mu_0) \exp\left(-\frac{\tau}{\mu_0}\right), \quad (4)$$

subject to the boundary conditions

$$I(0, \mu) = 0, \quad \mu < 0,$$

$$I(\tau_0, \mu) = 2\pi \int_{-1}^{0} I(\tau_0, \mu') r(\mu', \mu) |\mu'| \mathrm{d}\mu' + \pi F_0 \mu_0 r(-\mu_0, \mu) \exp\left(-\frac{\tau_0}{\mu_0}\right), \quad \mu > 0, \quad (5)$$

where $p(\mu, \mu')$ and $r(\mu', \mu)$ are the azimuth-independent phase function and the ground BRDF, respectively. They are defined as

$$p(\mu, \mu') = \frac{1}{2\pi} \int_0^{2\pi} P(\mu, \phi, \mu', \phi') \mathrm{d}\phi' = \sum_{l=0}^{3} \omega_l P_l(\mu) P_l(\mu'),$$

$$r(\mu', \mu) = \frac{1}{2\pi} \int_0^{2\pi} R(\mu', \phi', \mu, \phi) \mathrm{d}\phi'. \quad (6)$$

Here P_l are the Legendre polynomials of order l and are given in Appendix A. ω_l can be determined by

$$\omega_l = \frac{2l+1}{2}\int_{-1}^{1} p(x)P_l(x)\mathrm{d}x.$$

we thus obtain the final matrix equation for the coefficients L_j:

$$\mathbf{L} = \mathbf{A}^{-1}\mathbf{B}, \tag{9}$$

where

$$\mathbf{L} = [L_1, L_2, L_{-1}, L_{-2}]^T,$$

$$\mathbf{A} = \begin{bmatrix} W_1(-\mu_1) & W_2(-\mu_1) & W_1(\mu_1) & W_2(\mu_1) \\ W_1(-\mu_2) & W_2(-\mu_2) & W_1(\mu_2) & W_2(\mu_2) \\ [\alpha_{-1}(\mu_1) - W_1(\mu_1)]t_1 & [\alpha_{-2}(\mu_1) - W_2(\mu_1)]t_2 & \dfrac{\alpha_1(\mu_1) - W_1(-\mu_1)}{t_1} & \dfrac{\alpha_2(\mu_1) - W_2(-\mu_1)}{t_2} \\ [\alpha_{-1}(\mu_2) - W_1(\mu_2)]t_1 & [\alpha_{-2}(\mu_2) - W_2(\mu_2)]t_2 & \dfrac{\alpha_1(\mu_2) - W_1(-\mu_2)}{t_1} & \dfrac{\alpha_2(\mu_2) - W_2(-\mu_2)}{t_2} \end{bmatrix},$$

$$\mathbf{B} = (b_1, b_2, b_{-1}, b_{-2})^T.$$

Because of the presence of the integration term on the right-hand side of Eq. (4), no closed-form solution of Eq. (4) can be derived. Below, a two-stage approach is developed. In the first stage, the conventional four-stream approximation is extended to include a non-Lambertian boundary surface, yielding radiances at four Gaussian quadrature points. In the second stage, we derive radiances at arbitrary directions by approximating the integration term in Eq. (4) with the four-point formula. After the total azimuth-independent scattering radiance is calculated, the multiple-scattering component is then derived by subtraction of the azimuth-independent single-scattering radiance.

The four-stream discrete-ordinate solution to Eq. (4) at arbitrary level τ is given by[10,14]

$$I(\tau, x) = \sum_{j=1}^{2}[L_j W_j(x)\exp(-k_j\tau) + L_{-j}W_j(-x)\exp(k_j\tau)] + Z(x)\exp\left(-\frac{\tau}{\mu_0}\right), \tag{7}$$

where $x = \pm\mu_1$ (0.3399810), $\pm\mu_2$ (0.8611363) and functions $W_j(x)$, $Z(x)$, and k_j are known[10] and are given in Appendix A. L_j are coefficients to be determined based on the boundary conditions

$$I(0, x) = 0 \quad x = -\mu_{1,2}$$

$$I(\tau_0, x) = \frac{\pi}{0.52127}\sum_{j=1}^{2} a_j\mu_j r(-\mu_j, x)I(\tau_0, -\mu_j) + \mu_0\pi F_0 r(-\mu_0, x)\exp\left(-\frac{\tau_0}{\mu_0}\right) \quad x = \mu_{1,2}. \tag{8}$$

The explanation of the constant 0.52127 can be found in Ref. 11. a_1 (0.6521452) and a_2 (0.3478548) are the Gaussian weights. Substituting Eqs. (8) into Eq. (7), $[\cdot]^T$ denotes the matrix transpose, and the corresponding parameters are defined as

$$\alpha_{-1}(x) = \frac{\pi}{0.52127}\sum_{j=1}^{2} a_j\mu_j r(-\mu_j, x)W_1(-\mu_j),$$

$$\alpha_{-2}(x) = \frac{\pi}{0.52127}\sum_{j=1}^{2} a_j\mu_j r(-\mu_j, x)W_2(-\mu_j),$$

$$\alpha_1(x) = \frac{\pi}{0.52127}\sum_{j=1}^{2} a_j\mu_j r(-\mu_j, x)W_1(\mu_j),$$

$$\alpha_2(x) = \frac{\pi}{0.52127}\sum_{j=1}^{2} a_j\mu_j r(-\mu_j, x)W_2(\mu_j),$$

$$t_1 = \exp(-k_1\tau_0),$$

$$t_2 = \exp(-k_2\tau_0),$$

$$b_1 = -Z(-\mu_1),$$

$$b_2 = -Z(-\mu_2),$$

$$b_{-1} = -\left[\frac{\pi}{0.52127}\sum_{j=1}^{2} a_j\mu_j r(-\mu_j, \mu_1)Z(-\mu_j) + \mu_0\pi F_0 r(-\mu_0, \mu_1) - Z(\mu_1)\right]\exp\left(-\frac{\tau_0}{\mu_0}\right),$$

$$b_{-2} = -\left[\frac{\pi}{0.52127}\sum_{j=1}^{2} a_j\mu_j r(-\mu_j, \mu_2)Z(-\mu_j) + \mu_0\pi F_0 r(-\mu_0, \mu_2) - Z(\mu_2)\right]\exp\left(-\frac{\tau_0}{\mu_0}\right).$$

The inverse of the matrix $\mathbf{A}^{-1}$ can be calculated with any numerical calculation package. However, to avoid an unnecessary iteration process, an explicit formula for $\mathbf{L}_j$ is provided in Appendix B.

Now we need to find the solutions for arbitrary directions. Because the radiances at four Gaussian

quadrature points have been determined, one natural way of finding these solutions is to approximate the integration term in Eq. (4) with the four-point formula. Substituting Eq. (7) into Eq. (4), we show that Eq. (4) becomes an ordinary differential equation:

$$\mu \frac{dI(\tau, \mu)}{d\tau} - I(\tau, \mu) = -\frac{\omega}{2} \sum_{l=-2}^{2} a_l p(\mu, \mu_l) \left\{ \sum_{j=1}^{2} [L_j W_j(\mu_j) \exp(-k_j \tau) + L_{-j} W_j(-\mu_j) \exp(k_j \tau)] + Z(\mu_l) \exp\left(-\frac{\tau}{\mu_0}\right) \right\} - \frac{\omega}{4} F_0 p(\mu, -\mu_0) \exp\left(-\frac{\tau}{\mu_0}\right), \quad (10)$$

with boundary conditions (5). Solving Eq. (10), we have

$$I(\tau, \mu) = -\frac{\omega}{2} \sum_{l=-2}^{2} a_l p(\mu, \mu_l) \left\{ \sum_{j=1}^{2} \left[\frac{-L_j W_j(\mu_l)}{k_j \mu + 1} \exp(-k_j \tau) + \frac{L_{-j} W_j(-\mu_l)}{k_j \mu - 1} \exp(k_j \tau) \right] - \frac{Z(\mu_l) \mu_0}{\mu + \mu_0} \times \exp\left(-\frac{\tau}{\mu_0}\right) \right\} + \frac{\omega F_0 \mu_0 p(\mu, -\mu_0)}{4(\mu + \mu_0)} \times \exp\left(-\frac{\tau}{\mu_0}\right) + C(\mu) \exp\left(\frac{\tau}{\mu}\right) \quad (11)$$

for $\mu > 0$ and $\mu < 0$ but $|\mu| \neq \mu_0$. For the case of $\mu < 0$ and $|\mu| = \mu_0$, the radiance can be calculated:

$$I(\tau, \mu) = -\frac{\omega}{2} \sum_{l=-2}^{2} a_l p(\mu, \mu_l) \left\{ \sum_{j=1}^{2} \left[\frac{-L_j W_j(\mu_l)}{k_j \mu + 1} \exp(-k_j \tau) + \frac{L_{-j} W_j(-\mu_l)}{k_j \mu - 1} \exp(k_j \tau) \right] - \frac{Z(\mu_l) \tau}{\mu} \exp(\tau/\mu) \right\} - \frac{\omega F_0 \tau}{4\mu} p(\mu, -\mu_0) \exp(\tau/\mu) + C(\mu) \exp\left(\frac{\tau}{\mu}\right). \quad (12)$$

The coefficient $C(\mu)$ needs to be determined according to the boundary conditions (5). When $\mu < 0$ and $|\mu| \neq \mu_0$,

$$C(\mu) = \frac{\omega}{2} \sum_{l=-2}^{2} a_l p(\mu, \mu_l) \left\{ \sum_{j=1}^{2} \left[\frac{-L_j W_j(\mu_l)}{k_j \mu + 1} + \frac{L_{-j} W_j(-\mu_l)}{k_j \mu - 1} \right] - \frac{Z(\mu_l) \mu_0}{\mu + \mu_0} \right\} - \frac{\omega F_0 \mu_0 p(\mu, -\mu_0)}{4(\mu + \mu_0)}. \quad (13)$$

When $\mu < 0$ and $|\mu| = \mu_0$,

$$C(\mu) = \frac{\omega}{2} \sum_{l=-2}^{2} a_l p(\mu, \mu_l) \sum_{j=1}^{2} \left[\frac{-L_j W_j(\mu_l)}{k_j \mu + 1} + \frac{L_{-j} W_j(-\mu_l)}{k_j \mu - 1} \right]. \quad (14)$$

When $\mu > 0$,

$$C(\mu) = \frac{\omega}{2} \sum_{l=-2}^{2} a_l p(\mu, \mu_l) \left\{ \sum_{j=1}^{2} \left(\frac{-L_j W_j(\mu_l)}{k_j \mu + 1} \times \exp\left[-\left(k_j + \frac{1}{\mu}\right) \tau_0 \right] + \frac{L_{-j} W_j(-\mu_l)}{k_j \mu - 1} \times \exp\left[\left(k_j - \frac{1}{\mu}\right) \tau_0 \right] \right) - \frac{Z(\mu_l) \mu_0}{\mu + \mu_0} \times \exp\left[-\tau_0 \left(\frac{1}{\mu_0} + \frac{1}{\mu} \right) \right] \right\} - \frac{\omega F_0 \mu_0 p(\mu, -\mu_0)}{4(\mu + \mu_0)} \times \exp\left[-\tau_0 \left(\frac{1}{\mu_0} + \frac{1}{\mu} \right) \right] + I(\tau_0, \mu) \exp\left(-\frac{\tau_0}{\mu}\right), \quad (15)$$

where $I(\tau_0, \mu)$ is given in Eqs. (5).

Thus the multiple-scattering radiance with azimuth independence can be obtained as

$$I^{ms}(\tau, \mu) = I(\tau, \mu) - \bar{I}^{ss}(\tau, \mu), \quad (16)$$

where $\bar{I}^{ss}(\tau, \mu)$ is the azimuth-integrated single-scattering radiance, which has formulas the same as Eqs. (2) and (3) except that $P(\cdot)$ will be replaced with $p(\cdot)$.

4. Statistical BRDF of Land Surfaces

In a previous paper we provided a statistical BDRF that well represents measured directional reflectance of various ground covers.[8] This BRDF model can be expressed by

$$R(\Omega_i, \Omega) = f_1(\Omega_i, \Omega) + f_2(\Omega_i, \Omega), \quad (17)$$

where f_1 is a bowl-shaped component and f_2 is a hotspot (enhanced backscattering) component:

$$\begin{cases} f_1(\Omega_i, \Omega) = b_0 + b_1 \theta_i \theta \cos(\phi - \phi_i) + b_2 \theta_i^2 \theta^2 + b_3(\theta_i^2 + \theta^2) \\ f_2(\Omega_i, \Omega) = a_0 \exp[-a_1 \tan(\pi - \alpha)]. \end{cases} \quad (18)$$

In these expressions, α is the phase angle between the incident direction (μ_i, ϕ_i) and the outgoing direction (μ, ϕ). $\theta_i = \cos^{-1}(\mu_i)$; $\theta = \cos^{-1}(\mu)$; θ_i and ϕ_i are the incident zenith angle and the azimuth angle, respectively; and θ and ϕ are the viewing zenith angle and the azimuth angle, respectively. b_i and a_i are coefficients that fit functions f_2 and f_1. If the viewing direction coincides with the solar incidence, then $\alpha = \pi$ and $f_2(\cdot)$ approaches the local maximum.

The plane albedo $A(\mu_i)$ and the spherical albedo ρ

based on the present model can be calculated with

$$A(\mu_i) = \pi \int_{2\pi^-} [f_1(\Omega_i, \Omega) + f_2(\Omega_i, \Omega)]\mu d\Omega,$$

$$\rho = 2 \int_{-1}^{0} A(\mu_i)|\mu_i| d\mu_i, \tag{19}$$

respectively, where $2\pi^-$ represents the lower hemisphere.

5. Delta Scaling

It is also possible to incorporate a δ-function adjustment to account for the forward-scattering peak.[11,12,15] If a fraction of the scattering energy f is considered to be in the forward peak, the above solution can still be used as long as the following transformations are made in the coefficients:

$$\tau_0 \rightarrow \tau_0' = (1 - \omega f)\tau_0,$$

$$w_l \rightarrow \omega_l' = \frac{(1 - f)\omega_l}{1 - \omega_l f},$$

$$g \rightarrow g' = \frac{g - f}{1 - f}, \tag{20}$$

where g is the asymmetry parameter in a one-term Henyey–Greenstein function. Although various choices of f are possible,[15] $f = \omega_4/9$ has been used in the calculations below so that $\omega_l' = 0$ for $l \geq 4$. Notice that the scaling process is only for the calculation of multiple scattering.

6. Data Analysis

To validate the δ-four-stream formulas derived in Section 5, we calculate the upwelling radiance at the top of the aerosol atmosphere much more exactly with our Gauss–Seidel algorithm.[7] This Gauss–Seidel algorithm agrees with the discrete-ordinate algorithm,[6] with a relative error of 0.1–0.5% for the case of a Lambertian boundary surface. A major advantage of the Gauss–Seidel algorithm is that any form of BRDF for the non-Lambertian boundary surface can be easily incorporated without any extra computational cost.[7] In our trials the relative error is defined as $[\hat{I}(\tau, \Omega) - I(\tau, \Omega)]/I(\tau, \Omega) \times 100\%$, where $I(\tau, \Omega)$ and $\hat{I}(\tau, \Omega)$ are calculated with the Gauss–Seidel algorithm and the δ-four-stream approximation, respectively.

The parameters characterizing the ground BRDF are listed in Table 1. Both sets of parameters (albedos 0.1 and 0.3) are fitted from the ground-measured directional reflectance of a dense soybean canopy[16] in the green (500–600-nm) and the near-infrared (800–1100-nm) bands. However, these coefficients have been normalized to produce the specific albedo. Figure 1 illustrates the BRDF at an incident zenith angle of 30° and an azimuth angle of 0°. In the backscattering direction there is a local maximum, which is usually called the hotspot peak or the backscattering enhancement.

In the following calculations, only an aerosol atmosphere with a small optical depth is considered. If the optical depth is large, say, greater than 0.5, it is quite difficult to determine ground properties from satellite or aircraft imagery quantitatively. In practice, images that are from turbid atmospheres will not

Table 1. Parameters for the Statistical BRDF

	Parameter					
Albedo	b_0	b_1	b_2	b_3	a_0	a_1
0.10	−0.37532	0.00895	0.00275	0.01240	0.40356	0.03900
0.30	0.01277	0.00543	0.00064	0.02011	0.08012	0.41800

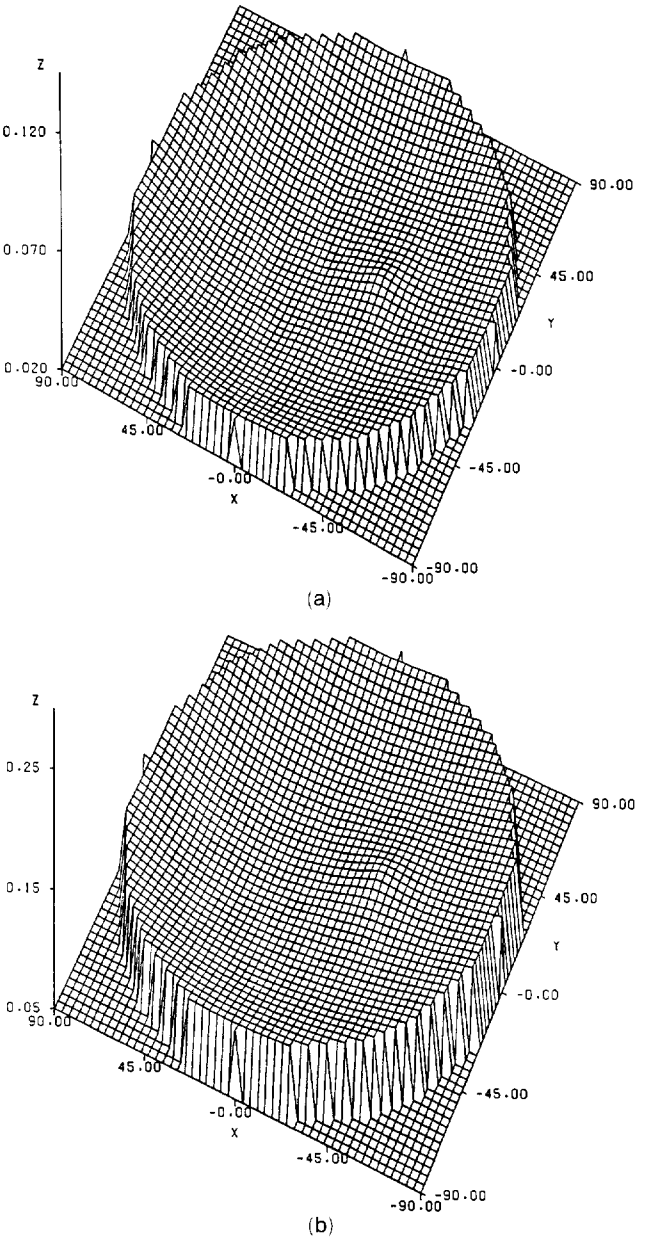

Fig. 1. Illustration of the BRDF for the non-Lambertian surface. The incident zenith angle is 30°, and the azimuth angle is 0°. (a) Albedo 0.1, (b) albedo 0.3. BRDF parameters are listed in Table 1.

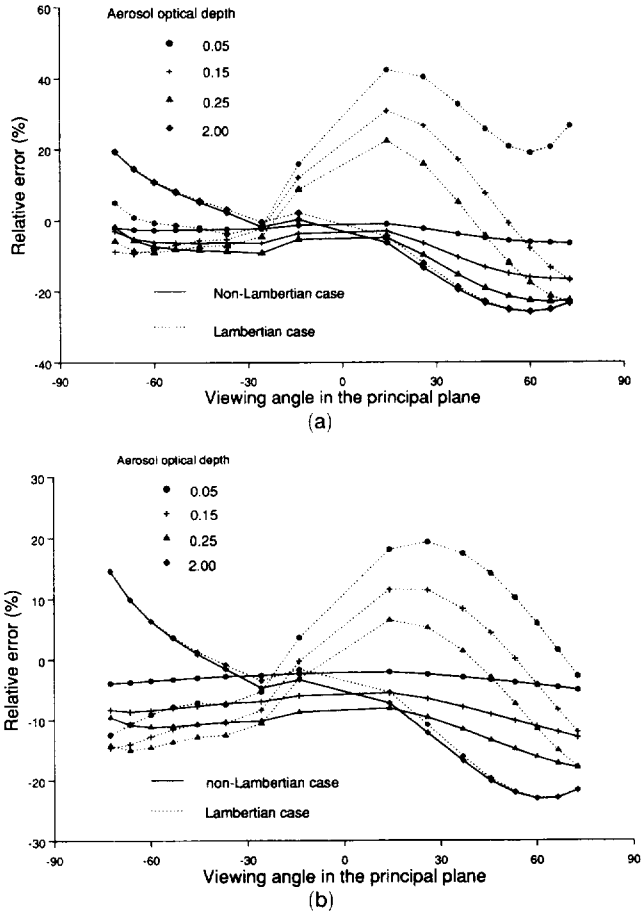

Fig. 2. Relative errors of the upwelling radiance in the principal plane with the δ-four-stream approximation. (a) Albedo 0.1, (b) albedo 0.3. Aerosol asymmetry parameter 0.75, single-scattering albedo of aerosol 0.96. The incident zenith angle is 30°, and the azimuth angle is 0°.

be used. Calculations with a Lambertian surface reflectance derived from the BRDF-integrated albedo are also implemented for comparisons, which provide information about the errors resulting from a Lambertian assumption for a non-Lambertian surface.

Figure 2 illustrates the relative errors of the upwelling radiance at the top of the atmosphere with the δ-four-stream approximation viewed in the principal plane. Figure 2(a) corresponds to the low-albedo (0.1) surface, and Fig. 2(b) corresponds to the high-albedo surface (0.3). The aerosol asymmetry parameter is also different: 0.65 in Fig. 2(a) and 0.75 in Fig. 2(b). From Fig. 2 we can see that for the non-Lambertian surface, a Lambertian assumption can lead to large errors, especially in the forward-scattering direction and in clearer atmospheres. When the aerosol optical depth is between 0.05–0.25, the δ-four-stream approximation yields increasing errors as optical depth increases. The approximation seems to underestimate the upwelling radiance in all cases, which is consistent with the calculations of Liou *et al.*[12] in the Lambertian case. At an optical depth of 2.0, the model overestimates the upwelling radiance in the backscattering direction and underestimates the upwelling radiance in the forward direction. The reason is probably the azimuth-independent approximation for the multiple-scattering component. In this case multiple scattering becomes large and there is stronger forward scattering than backward scattering. At this optical depth, it can also be observed that the Lambertian assumption produces radiances close to the non-Lambertian and close to the Gauss–Seidel results as well. This is due to the strong multiple interactions between the atmo-

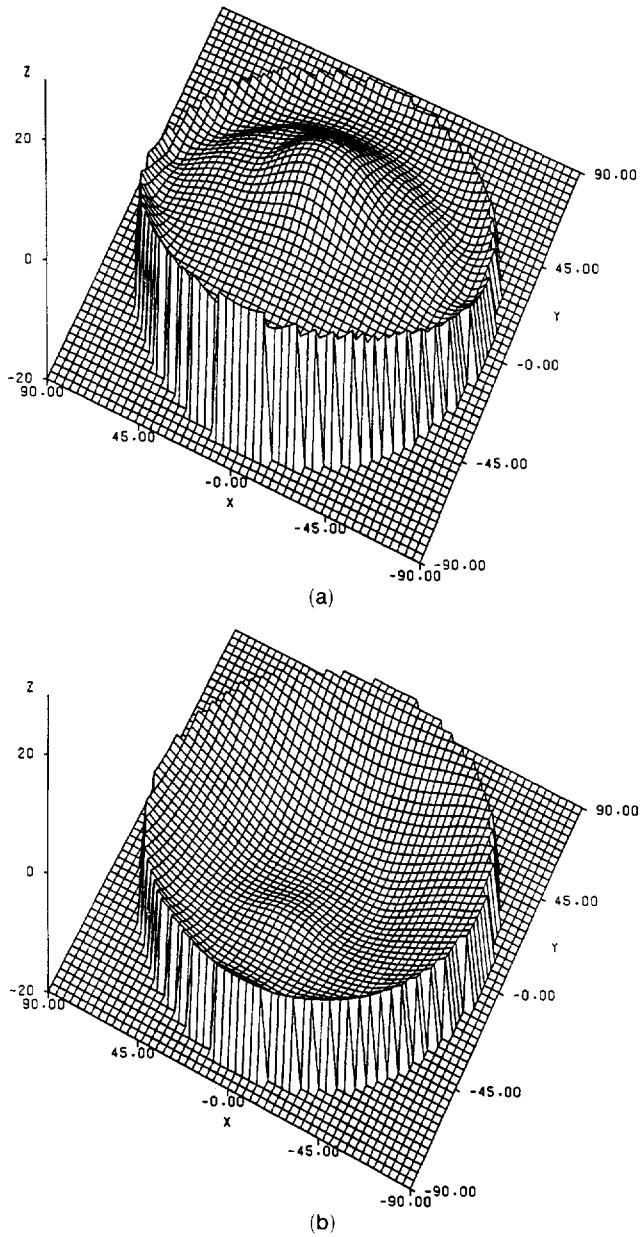

Fig. 3. Relative errors of the upwelling radiance with the δ-four-stream approximation, displayed as a three-dimensional surface in the three-dimensional coordinate. The optical depth is 0.15. (a) Albedo 0.1, (b) albedo 0.3. The other parameters are the same as in Fig. 2. The zenith and azimuth viewing angles are resolved into x and y coordinates, respectively, and the height of the surface displays the percentage error at that viewing position. The plane $y = 0$ is the principal plane.

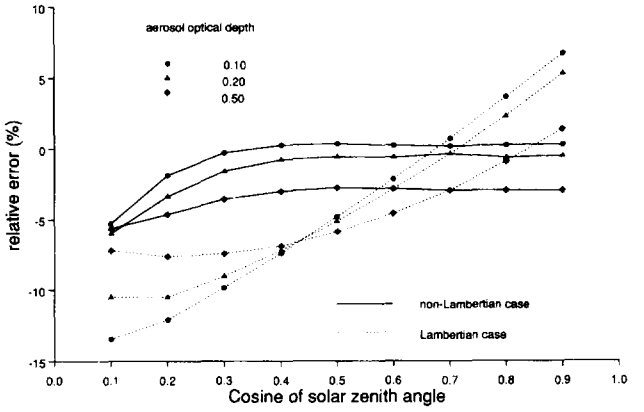

Fig. 4. Relative errors in the upwelling radiative flux as a function of illumination zenith angle. Albedo 0.3, aerosol asymmetry parameter 0.75, single-scattering albedo of aerosol 0.96.

sphere and the surface. Notice that if the viewing angle is smaller than 30°, the δ-four-stream approach predicts the upwelling radiance with a relative error smaller than 10% over the full range of the optical depths.

Relative errors outside of the principal plane for the δ-four-stream approximation with the non-Lambertian surface are presented in Fig. 3 as a three-dimensional graphic. Because the errors are asymmetrical in azimuth, an azimuth-dependent approximate solution for the multiple-scattering radiance should be developed if higher accuracy is sought.

Figure 4 presents the effects of the improved δ-four-stream approximation on the calculation of the upwelling radiative flux. Although the improved δ-four-stream approximation underestimates the flux a little, it obviously has a higher accuracy than the Lambertian assumption. The relative error is smaller than 5%.

One of the major objectives of this study is to develop analytical atmospheric radiative transfer models for multiangle remotely sensed data, such as the

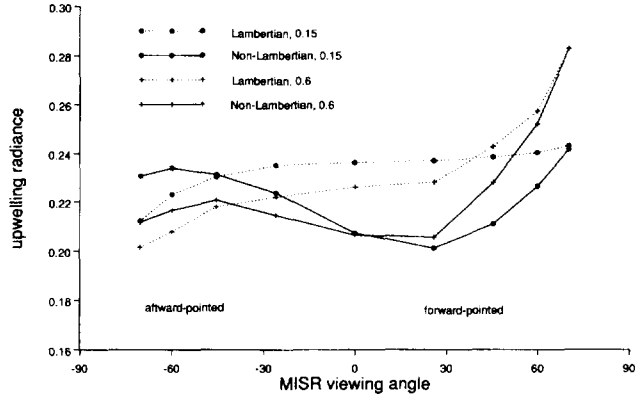

Fig. 5. Effects of the assumption of a Lambertian surface on upwelling radiance at the MISR viewing positions calculated with the Gauss–Seidel algorithm. Albedo 0.3, aerosol asymmetry parameter 0.75, single-scattering albedo of aerosol 0.90, $\mu_0 = 0.81$. The forward observation plane lies in $\phi_0 + 48°$, and the aftward observation plane lies in $\phi_0 + 132°$.

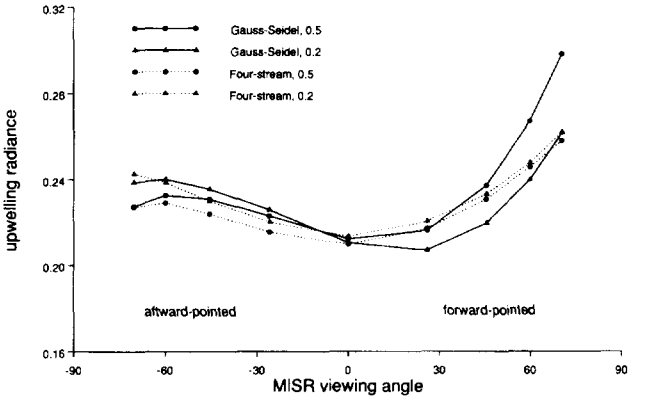

Fig. 6. Comparison of the upwelling radiance in the MISR viewing angles calculated with the Gauss–Seidel algorithm and with the δ-four-stream approximation. Aerosol asymmetry parameter 0.65, single-scattering albedo of aerosol 0.94. The other parameters are the same as in Fig. 5.

Multiangle Imaging Spectroradiometer (MISR). The MISR consists of nine cameras, of which four point in the forward direction, four point in the aftward direction, and one points in the nadir direction. Figure 5 illustrates the effects of the assumption of a Lambertian surface on the upwelling radiances at nine MISR directions (latitude 30°, 21 March) calculated with the Gauss–Seidel algorithm. In the case of the non-Lambertian surface, the upwelling radiance has a larger angular variation than in the Lambertian case. Furthermore, the Lambertian assumption produces larger errors at small optical depths. Because we are more interested in the clear atmosphere case for remote sensing of Earth resources, the proper incorporation of the non-Lambertian surface into the atmospheric radiance transfer formulation is of great importance.

Figure 6 compares the upwelling radiance calculated with the Gauss–Seidel algorithm and the four-stream approximation at nine MISR directions (latitude 30°, 21 March) with two aerosol optical depths. The four-stream approximation overestimates the upwelling radiance in forward directions to some degree and underestimates the upwelling radiance in aftward directions somewhat as well. Note that the forward–aftward plane, which is controlled by the planned orbit of the Earth Observing System AM platform, is not in the solar principal plane. However, the four-stream non-Lambertian approximation still fits the Gauss–Seidel numerical solution much better than a Lambertian model.

From the above results, it can be concluded that incorporating ground BRDF into the analytical δ-four-stream formula can significantly improve the accuracy of the upwelling radiance calculation for a non-Lambertian boundary surface.

7. Discussion and Conclusion

The conventional four-stream approximation for radiative flux has been extended to calculate the angular radiance distribution over a non-Lambertian surface. The Gauss–Seidel numerical code is applied to

examine the accuracy of the improved four-stream algorithm. The results show that the new model predicts the radiance as well as radiative flux quite well. The Lambertian assumption could lead to large errors for non-Lambertian boundary conditions. The new four-stream algorithm predicts the upwelling radiance at small viewing angles better than at large viewing angles. However, this may not be much of a disadvantage, because most existing and planned remote sensors for Earth resource investigations are nadir viewing or view in the near-nadir directions.

The four-stream model is very computationally efficient. We compared the four-stream code with the Gauss–Seidel code on a SPARC-10 workstation with the same set of parameters (see Fig. 6). The Gauss–Seidel code took approximately 14.45 s to calculate radiance at 64 directions, but the four-stream code took approximately 0.08 s.

The science community strongly desires efficient algorithms for quick calculations. LOWTRAN and 6S have been widely used for remote sensing and environmental optics, but both are based on two-stream approximations. Although no comparisons with LOWTRAN or 6S are implemented in this paper, the four-stream algorithm should improve the approximation of multiple scattering. In some cases such as atmospheric correction of satellite imagery, approximate models are suitable if atmospheric parameters are empirically estimated. We also notice that in some cases the accuracy of the present model is not satisfactory, and further improvements are still needed. For example, in the present formulation, the multiple-scattering radiance is assumed to be azimuth independent. For a clear atmosphere, multiple scattering usually is asymmetric in the azimuth direction. To improve the accuracy of the present algorithm, further research that considers the azimuthal dependence of multiple scattering is required. Fourier transformation obviously is one possible technique for this purpose.

A desirable objective for remote sensing is the retrieval of the ground BRDF from multiangle remotely sensed data. Further research relating to the present modeling effort in the near future will explore the possibility of retrieval of the BRDF, provided that atmospheric parameters are known. The important issue is to observe the effects of the prediction errors of the four-stream model on the BRDF retrieval and to test the sensitivity of the model to various possible noise sources.

Appendix A: Ancillary Functions

$$W_{1,2}(x) = \frac{1}{1 + k_{1,2}x} \sum_{l=0}^{3} \omega_l \xi_l(k_{1,2}) P_l(x),$$

$$Z(x) = \frac{\mu_0 F_0}{4(\mu_0 + x)} \frac{(\mu_1^2 - \mu_0^2)(\mu_2^2 - \mu_0^2)}{\mu_1^2 \mu_2^2 (1 - k_1^2 \mu_0^2)(1 - k_2^2 \mu_0^2)} \times \sum_{l=0}^{3} \omega_l \xi_l \left(\frac{1}{\mu_0}\right) P_l(x).$$

The Legendre polynomials and ξ functions for an argument x are listed as follows:

$$P_0(x) = 1,$$

$$P_1(x) = x,$$

$$P_2(x) = \frac{1}{2}(3x^2 - 1),$$

$$P_3(x) = \frac{1}{2}(5x^3 - 3x),$$

$$P_4(x) = \frac{7}{4} x P_3(x) - \frac{3}{4} P_2(x),$$

$$\xi_0(x) = 1,$$

$$\xi_1(x) = -\frac{(1 - \omega_0^*)}{x},$$

$$\xi_2(x) = \frac{(3 - \omega_1^*)(1 - \omega_0^*)}{2x^2} - \frac{1}{2},$$

$$\xi_3(x) = -\frac{(5 - \omega_2^*)(3 - \omega_1^*)(1 - \omega_0^*)}{6x^3} + \frac{5 - \omega_2^* + 4(1 - \omega_0^*)}{6x}.$$

The eigenvalues k_1 and k_2 can be determined from

$$k^2 = -\frac{b}{2} \pm \frac{1}{2}(b^2 - 4c)^{1/2},$$

where

$$b = \frac{a_1 t_1 - 1}{\mu_1^2} + \frac{a_2 t_2 - 1}{\mu_2^2},$$

$$c = \frac{1 - a_1 t_1 - a_2 t_2}{\mu_1^2 \mu_2^2} + \frac{a_1 t_1'}{\mu_1^2} + \frac{a_2 t_2'}{\mu_2^2},$$

$$t_{1,2} = \omega_0^* + \omega_1^*(1 - \omega_0^*)\mu_{1,2} - \frac{\omega_2^*}{2} P_2(\mu_{1,2}) - \frac{\omega_3^*}{6}[(5 - \omega_2^*) + 4(1 - \omega_0^*)]\mu_{1,2} P_3(\mu_{1,2}),$$

$$t_{1,2}' = \frac{1}{2}(3 - \omega_1^*)(1 - \omega_0^*)[\omega_2^* P_2(\mu_{1,2}) + \frac{\omega_3^*}{3}(5 - \omega_2^*)\mu_{1,2} P_3(\mu_{1,2})].$$

ω_l^* can be determined by the following:

$$\omega_l^* = \omega \omega_l.$$

If δ scaling is used, then

$$\omega_l^* \rightarrow \varpi_l = \frac{\omega_l^* - f(2l + 1)}{1 - f}.$$

Appendix B: Explicit Solution of a Four-Dimensional Linear Equation Set

Suppose that we need to solve this set of equations:

$$[\mathbf{a}_1\ \mathbf{a}_2\ \mathbf{a}_3\ \mathbf{a}_4]\mathbf{x} = \mathbf{b},$$

where

$$\mathbf{a}_1 = [a_{11}\ a_{21}\ a_{31}\ a_{41}]^T,$$
$$\mathbf{a}_2 = [a_{12}\ a_{22}\ a_{32}\ a_{42}]^T,$$
$$\mathbf{a}_3 = [a_{13}\ a_{23}\ a_{33}\ a_{43}]^T,$$
$$\mathbf{a}_4 = [a_{14}\ a_{24}\ a_{34}\ a_{44}]^T,$$
$$\mathbf{x} = [x_1\ \ x_2\ \ x_3\ \ x_4]^T,$$
$$\mathbf{b} = [b_1\ \ b_2\ \ b_3\ \ b_4]^T.$$

It follows that

$$x_k = \frac{\Delta_k}{\Delta},$$

where

$$\Delta_1 = |\mathbf{b}\ \ \mathbf{a}_2\ \mathbf{a}_3\ \mathbf{a}_4|,$$
$$\Delta_2 = |\mathbf{a}_1\ \mathbf{b}\ \ \mathbf{a}_3\ \mathbf{a}_4|,$$
$$\Delta_3 = |\mathbf{a}_1\ \mathbf{a}_2\ \mathbf{b}\ \ \mathbf{a}_4|,$$
$$\Delta_4 = |\mathbf{a}_1\ \mathbf{a}_2\ \mathbf{a}_3\ \mathbf{b}|,$$
$$\Delta = |\mathbf{a}_1\ \mathbf{a}_2\ \mathbf{a}_3\ \mathbf{a}_4|,$$

and where $|\cdot|$ is the determinant of the 4×4 matrix. The determinants can be easily calculated, for instance for Δ, as follows:

$$\Delta = a_{11}M_{11} - a_{21}M_{21} + a_{31}M_{31} - a_{41}M_{41},$$

where

$$M_{11} = \begin{vmatrix} a_{22} & a_{23} & a_{24} \\ a_{32} & a_{33} & a_{34} \\ a_{42} & a_{43} & a_{44} \end{vmatrix}, \quad M_{21} = \begin{vmatrix} a_{12} & a_{13} & a_{14} \\ a_{32} & a_{33} & a_{34} \\ a_{42} & a_{43} & a_{44} \end{vmatrix},$$

$$M_{31} = \begin{vmatrix} a_{12} & a_{13} & a_{14} \\ a_{22} & a_{23} & a_{24} \\ a_{42} & a_{43} & a_{44} \end{vmatrix}, \quad M_{41} = \begin{vmatrix} a_{12} & a_{13} & a_{14} \\ a_{22} & a_{23} & a_{24} \\ a_{32} & a_{33} & a_{34} \end{vmatrix},$$

and the determinant of each 3×3 matrix can be explicitly calculated from elementary formulas.

This work was supported in part by NASA under grant NAGW-2082 and contracts NAS5-30917 and NAS5-31369 and by the National Science Foundation under grant INT-9014263. The authors thank David Diner for providing the MISR viewing-angle data and an anonymous reviewer for his provocative comments.

References

1. J. R. Irons, K. J. Ranson, D. L. Williams, R. R. Irish, and F. G. Huegel, "An off-nadir pointing imaging spectroradiometer for terrestrial ecosystem studies," IEEE Trans. Geosci. Remote Sensing **29,** 66–74 (1991).
2. D. J. Diner, C. J. Bruegge, J. V. Martonchik, T. P. Ackerman, R. Davies, S. A. W. Gerstl, H. R. Gordon, P. J. Sellers, J. Clark, J. A. Damiels, E. D. Danielson, V. G. Duval, K. P. Klaasen, G. W. Lilienthal, D. I. Nakamoto, R. J. Pagano, and T. H. Reilly, "MISR: a multiangle imaging spectroradiometer for geophysical and climatological research for EOS," IEEE Trans. Geosci. Remote Sensing **27,** 200–214 (1989).
3. D. J. Diner and J. V. Martonchik, "Atmospheric transfer of radiation above an inhomogeneous non-Lambertian reflective ground. I. Theory," J. Quant. Spectrosc. Radiat. Transfer **31,** 97–125 (1984).
4. D. J. Diner and J. V. Martonchik, "Atmospheric transfer of radiation above an inhomogeneous non-Lambertian reflective ground. II. Computational considerations and results," J. Quant. Spectrosc. Radiat. Transfer **32,** 279–304 (1984).
5. T. Lee and Y. J. Kaufman, "The effect of surface nonlambertian on remote sensing of surface reflectance and vegetation index," IEEE Trans. Geosci. Remote Sensing **24,** 699–708 (1986).
6. K. Stamnes, S. C. Tsay, W. Wiscombe, and K. Jayaweera, "Numerically stable algorithm for discrete-ordinate-method radiative transfer in multiple scattering and emitting layered media," Appl. Opt. **27,** 2502–2509 (1988).
7. S. Liang and A. H. Strahler, "Calculation of the angular radiance distribution for a coupled atmosphere and canopy," IEEE Trans. Geosci. Remote Sensing **31,** 491–502 (1993).
8. S. Liang and A. H. Strahler, "Retrieval of surface BRDF from multiangle remotely sensed data," Remote Sensing Environ. to be published.
9. W. Verhoef, "A scene radiation model based on four stream radiative transfer theory," presented at the Third Colloquium on Spectral Signatures of Objects in Remote Sensing, Les Ares, France, 1985).
10. K. N. Liou, "Analytic two-stream and four-stream solutions for radiative transfer," J. Atmos. Sci. **31,** 1473–1475 (1974).
11. J. N. Cuzzi, T. P. Ackerman, and L. C. Helmle, "The delta-four-stream approximation for radiative flux transfer," J. Atmos. Sci. **39,** 917–925 (1982).
12. K. N. Liou, Q. Fu, and T. P. Ackerman, "A simple formulation of the delta-four-stream approximation for radiative transfer parameterizations," J. Atmos. Sci. **45,** 1940–1947 (1988).
13. J. Lenoble, *Radiative Transfer in Scattering and Absorbing Atmospheres: Standard Computational Procedures* (Deepak, Hampton, Va., 1985).
14. S. Chandrasekar, *Radiative Transfer* (Oxford U. Press, London, 1960).
15. J. H. Joseph, W. J. Wiscombe, and J. A. Weinman, "The delta-Eddington approximation for radiative flux transfer," J. Atmos. Sci. **33,** 2453–2459 (1976).
16. K. J. Ranson, L. L. Biehl, and C. S. T. Daughtry, "Soybean canopy reflectance modeling data sets," LARS Tech. Rep. 071584 (Laboratory for Applications of Remote Sensing, Purdue University, Lafayette, Ind., 1984).